Aquaculture Reports 48 (2026) 103676

Contents lists available at ScienceDirect

Aquaculture Reports

journal homepage: www.elsevier.com/locate/aqrep

Ampelopsis japonica enhances the resistance of Chinese soft-shelled turtles (*Pelodiscus sinensis*) to *Aeromonas veronii* by inhibiting bacterial infection

Jicheng Yang [a,1], Mengyuan Li [a,1], Jun Hu [a,b], Ruixiang Zhai [a], Shujie Guo [a], Zhirui Zhu [a], Beijuan Hu [a], Junhua Wang [a], Daxian Zhao [a], Zhongguo Li [c], Kou Peng [a,*], Yijiang Hong [a,*]

[a] Key Laboratory for Aquatic Germplasm Innovation and Utilization of Jiangxi Province, School of Life Sciences, Nanchang University, Nanchang 330031, China
[b] Xuanhan County Bureau of Agriculture and Rural Affairs, Dazhou, Sichuan 636150, China
[c] Nanfeng County Bureau of Agriculture and Rural Affairs, Fuzhou, Jiangxi 344500, China

ARTICLE INFO

Keywords:
Ampelopsis japonica
Chinese soft-shelled turtle
Aeromonas veronii
Intestinal health
Complement and coagulation cascades

ABSTRACT

Ampelopsis japonica (AJ) is an effective antibacterial agent widely used in humans and animals. However, the application of AJ in aquaculture animals remains largely unknown. In this study, we investigated the in vitro antibacterial activity of AJ against *Aeromonas veronii* (*A. veronii*) and evaluated its effects as a dietary supplement on intestinal health and disease resistance in Chinese soft-shelled turtles. The results showed that AJ significantly inhibited the growth of *A. veronii* and reduced the expression of virulence genes in vitro at a concentration of 25 mg/mL. Dietary supplementation with AJ at 1250 mg/kg significantly enhanced T-AOC and sIgA levels while reducing MPO and NO levels, as well as the expression of proinflammatory cytokines (TNF-α, IL-6, and IL-18), thereby promoting immune homeostasis. Furthermore, following *A. veronii* challenge, AJ supplementation maintained intestinal barrier integrity, sustained sIgA secretion, and reduced apoptosis by mitigating excessive inflammation and oxidative damage. In addition, AJ supplementation increased the expression of complement and coagulation related genes (*F3*, *F5*, *FGG*, *C3*, and *C9*), promoting the formation of membrane attack complexes (MAC, C5b-9) to eliminate pathogens. Overall, these findings indicate that AJ can be used as a functional feed additive to improve intestinal health and enhance resistance to *A. veronii* infection in Chinese soft-shelled turtles.

1. Background

Over recent decades, high-density intensive farming has become the dominant model in aquaculture, rendering farmed species increasingly vulnerable to pathogenic bacteria (Lieke et al., 2020). Frequent outbreaks of bacterial diseases, coupled with high mortality rates, pose significant challenges to sustainable aquaculture development and inflict substantial economic losses (Dadar et al., 2017). Chinese soft-shelled turtle (*Pelodiscus sinensis*), is an important aquaculture species in China, which is popular among consumers for its high nutritional and medicinal value (Chen et al., 2014). Numerous studies of bacterial diseases of Chinese soft-shelled have been reported, such as infectious diseases caused by *Aeromonas veronii* (*A. veronii*), *Bacillus cereus*, and *Morganella morganii* (Hu et al., 2023; Xiao et al., 2024; Zhai et al., 2024), which have severely constrained industry growth. Among them, *A. veronii* is the most common bacterium, widely distributed in aquatic environments and animals (Dien et al., 2022), and is one of the major pathogens in Chinese soft-shelled turtles (Dai et al., 2022). Currently, relevant studies have shown that the pathogenicity of *A. veronii* is closely related to many virulence factors, such as aerolysin, hemolysin, extracellular protease and S-layer protein, which cause systemic congestion, tissue damage, and immune system damage, leading to severe diseases (Kay et al., 1981; Lowry et al., 2014; Sen and Lye, 2007).

Multiple strategies, including probiotics, vaccines, immunostimulants, and Chinese herbal medicine, are currently applied to mitigate disease outbreaks and enhance growth performance in aquaculture (Liu et al., 2015). Chinese herbal medicines, rich in bioactive compounds (Schuhladen et al., 2019), have gained attention as sources of natural therapeutics with multifaceted functions: growth promotion (Amin et al., 2019), stress mitigation (Gharaei et al., 2020), immunomodulation (Abd El-Gawad et al., 2020), and antimicrobial activity (AftabUddin et al., 2017). Current studies have widely demonstrated that various bioactive constituents in Chinese herbal medicines, including essential

* Corresponding authors.
E-mail addresses: pengkou@126.com (K. Peng), yjhong@ncu.edu.cn (Y. Hong).
[1] These authors contributed equally to this work.

https://doi.org/10.1016/j.aqrep.2026.103676
Received 25 February 2026; Received in revised form 5 May 2026; Accepted 18 May 2026
Available online 22 May 2026

oils, saponins, phenolics, tannins, alkaloids, polypeptides, and polysaccharides (Hoseinifar et al., 2020), possess broad-spectrum antibacterial properties against various common aquatic pathogens (Elumalai et al., 2020). Beyond their direct antimicrobial efficacy, these compounds effectively modulate host immune responses; they act directly on immune organs to drive antibody production and specific immunity, while also stimulating cytokine generation to comprehensively modulate both specific and non-specific immune responses (Tadese et al., 2022).

In contrast to passive antibiotic interventions, these herbal therapeutics offer a proactive defense strategy by enhancing the host's intrinsic defenses (Elumalai et al., 2020; Zhang et al., 2022). In complex aquatic environments with high pathogen loads, relying solely on bacteriostatic approaches is often insufficient; therefore, the rapid activation of the host's innate immune network is imperative (Bondad-Reantaso et al., 2023). The complement system and the coagulation cascade represent two pivotal pathways within the innate immune system (Meng et al., 2025). Beyond their respective independent functions in pathogen clearance and physical sequestration, these two systems establish a synergistic molecular network known as "immunothrombosis" (Engelmann and Massberg, 2013). Within this network, coagulation factors can bypass the classical pathway to directly cleave and activate core complement components (C3/C5). Reciprocally, complement activation products, such as C5a and the membrane attack complex (MAC), strongly induce tissue factor (TF) expression and promote coagulation, thereby efficiently entrapping and eradicating pathogens during early localized infections (Foley and Conway, 2016).

Ampelopsis japonica (AJ), a traditional Chinese herbal medicine, clears heat, detoxifies, reduces swelling, dissipates nodules, promotes tissue regeneration, and relieves pain (Liang et al., 2022). Its diverse pharmacological properties are supported by the presence of numerous bioactive compounds, such as gallic acid, polysaccharides, and emodin derivatives (Zhu et al., 2024). Modern pharmacological studies have shown that AJ has anti-inflammatory, antioxidant, immunomodulatory, antibacterial, wound-healing, and antitumor effects (Lee et al., 2022; Oh et al., 2022). Notably, previous studies have shown that specific constituents like rhein, gallic acid, and emodin can effectively activate the complement system through the classical and alternative pathways (Zhong et al., 2024). However, it remains largely unknown whether dietary supplementation with AJ can effectively alleviate bacteria-induced intestinal inflammation in aquatic animals by modulating the complement and coagulation cascades.

This study aimed to investigate the direct inhibitory effect of AJ against *A. veronii* and to evaluate the effect of dietary AJ supplementation on the intestines of Chinese soft-shelled turtles, including its effect on survival, antioxidant, histopathology, and immune modulation, as well as the association of these effects with host resistance to *A. veronii* infection. Additionally, we explored the underlying mechanisms of the relevant regulatory pathways.

2. Materials and methods

2.1. Experimental design and protocol

A total of 120 healthy Chinese soft-shelled turtle, with an average body weight of 300 ± 50 g, were selected from a farm in Nanfeng County, Jiangxi Province, People's Republic of China. A total of twelve 1000-L round tanks were used, with the turtles randomly allocated to four treatment groups (control-C, AJ-supplemented-C+AJ, infected-I, and infected with AJ supplementation-I+AJ) in a design of three tanks per group (Table 1). The Chinese soft-shelled turtles were acclimatized in round tanks for one week without feeding. Following this period, they were fed the diets twice daily (at 08:00 and 17:00) for two weeks at a total daily rate of 3% of their body weight. Based on previous unpublished data from our laboratory evaluating dietary levels of 500, 750, 1000, 1250, and 1500 mg/kg, the 1250 mg/kg supplementation level demonstrated the best protective effect and was therefore selected for the AJ supplemented group in the present study. They were maintained in a static water system at a temperature of 28 ± 1 °C throughout the experimental period.

Table 1
Experimental grouping situation.

Group	Number	Feed	Injection Situation
C	30	Ordinary feed	sterile physiological saline
C+AJ	30	1250 mg/kg *Ampelopsis japonica* feed	sterile physiological saline
I	30	Ordinary feed	*Aeromonas veronii* infection
I+AJ	30	1250 mg/kg *Ampelopsis japonica* feed	*Aeromonas veronii* infection

Briefly, 3 g of the AJ extract (obtained from the Jiangxi Academy of Agricultural Sciences) was dissolved in 15 mL of sterile distilled water to prepare a solution with a final concentration of 200 mg/mL. After complete dissolution, the solution was sterilized by filtration through a 0.45 μm sterile filter membrane. The sterilized solution was stored at 4°C for future experiment.

2.2. Determination of minimum inhibitory concentration (MIC), minimum bactericidal concentration (MBC) and growth curve

A two-fold dilution method was used to prepare the drug concentration gradient, with final concentrations of 100, 50, 25, 12.5, 6.25, and 3.125 mg/mL in tubes 1–6. A 4 μL aliquot of bacterial suspension (6×10^8 CFU/mL) was inoculated into each of tubes 1–7. Tubes 1–6 served as experimental groups, tube 7 as a positive control (bacterial culture without drug), and tube 8 as a negative control (sterile medium only). Each treatment was performed in triplicate (labeled A, B, and C). The cultures were incubated at 28°C with 200 rpm agitation in a shaking incubator for 18–24 h. Bacterial growth inhibition was defined as OD600 < 0.05. The MIC value was determined as the lowest drug concentration demonstrating no visible bacterial growth.

Following the MIC assay, 100 μL aliquots from each EP tube were aseptically transferred to sterile LB agar plates, spread evenly using a sterile spreading rod, and then incubated inverted at 28°C for 24 h. The MBC value was defined as the lowest drug concentration at which no bacterial colonies were observed on the corresponding agar plate.

The growth curves of *A. veronii* were determined based on the MIC value by the AJ extract concentration corresponding to the MIC. A bacterial suspension with a concentration of 6×10^8 CFU/mL was prepared. The suspension was inoculated into LB liquid medium containing the AJ extract (Av + AJ) at a 1:100 (v/v) inoculum ratio, while LB medium without the extract was served as the control group (Av). Cultures were incubated at 28°C with 200 rpm agitation for 24 h. At 1-hour intervals, the OD600 values were measured using a microplate reader. Triplicate experiments were performed for each treatment group.

2.3. Strain source, culture, infection, and sample collection procedures

The bacterial strain used in this study, originally isolated from a diseased Chinese soft-shelled turtle, was stored in our laboratory and confirmed as *Aeromonas veronii* (*A. veronii*) through 16S rRNA sequencing. The median lethal dose (LD_{50}) was determined in a preliminary trial prior to the formal challenge. Healthy turtles were intraperitoneally injected with bacterial suspensions at concentrations ranging from1.0×10^7–1.0×10^9 CFU/mL, at a standardized dose of 0.1 mL per 100 g of body weight. Mortality was recorded daily for 14 days, and the LD_{50} was calculated as 6×10^8 CFU/mL using the Reed-Muench method. Subsequently, this LD_{50} value served as the basis for the dosage utilized in the formal infection model to evaluate the protective effects of dietary AJ. To prepare the inoculum for the formal

challenge evaluating the protective effects of dietary AJ, a 1% (v/v) *A. veronii* culture was transferred into 20 mL of sterile LB liquid medium and incubated at 28 °C with 200 rpm shaking for 6 h. The bacteria were harvested by centrifugation at 4000 rpm for 15 min, washed three times with 0.85% sterile physiological saline to remove residual medium, and resuspended to the predefined LD50 concentration (6 $\times 10^8$ CFU/mL). During the challenge assay, each turtle was intraperitoneally injected with this suspension (0.1 mL/100 g body weight), while the control group received an equivalent volume of 0.85% sterile saline following the same protocol. Mortality and clinical symptoms were monitored and recorded every 6 h post-infection. At 24 h post-infection, three Chinese soft-shelled turtles were euthanized from each group. Posterior intestine tissues were aseptically collected, divided into two parts, and preserved either in 4% paraformaldehyde solution or snap-frozen in liquid nitrogen. All procedures involving the handling of turtles were conducted in strict compliance with the regulations of the Animal Center of Nanchang University, China, and the sampling protocols received ethical approval from the Animal Care and Use Committee of the School of Life Sciences at Nanchang University (Approval ID: SYXK(GAN)2021–0004). Prior to any invasive procedures or tissue sampling, the turtles were deeply anesthetized using an immersion bath of MS-222. Following the loss of equilibrium and reflexivity, euthanasia was confirmed by decapitation before rapid tissue collection. All efforts were meticulously undertaken to ensure ethical compliance and minimize the turtles' suffering.

2.4. Measurement of pro-inflammatory cytokine and antioxidant parameters

The activity of total antioxidant capacity (T-AOC), myeloperoxidase (MPO) and nitric oxide (NO) were analyzed by following the protocols of the kits (Nanjing Jiancheng Bioengineering Institute, Nanjing, China).

The concentrations of tumor necrosis factor-α (TNF-α), interleukin-6 (IL-6), and interleukin-18 (IL-18) in both the supernatants of intestinal tissue homogenates and the lavage fluid for secretory immunoglobulin A (sIgA) were quantified in Chinese soft-shelled turtles using species-specific enzyme-linked immunosorbent assay (ELISA) kits (Yansheng Biotechnology Co., Ltd., China). Prior to formal sample analysis, all commercial ELISA kits were validated for use in Chinese soft-shelled turtle. Serial dilution tests of tissue homogenates were conducted to confirm that the sample optical density (OD) values fell within the linear range of the standard curves. Assay accuracy and precision were strictly monitored, with both intra-assay and inter-assay coefficients of variation (CV) maintained at < [15%]

2.5. Histological staining and apoptosis analysis

Following fixation in 4% paraformaldehyde, intestinal tissues were dehydrated with a graduated ethanol series and embedded in paraffin. Serial longitudinal (3–5μm thick) paraffin sections were subsequently obtained and placed onto adhesive-coated slides. After deparaffinization and rehydration, the sections were stained with Harris hematoxylin and eosin and examined using a Nikon NI-CTLB microscope.

Cell apoptosis in intestinal tissue sections (not subjected to hematoxylin and eosin (H&E) staining) was analyzed using the terminal deoxynucleotidyl transferase dUTP nick end labeling (TUNEL) BrightRed Apoptosis Detection Kit (Vazyme Biotech Co., Ltd., China), following the manufacturer's protocols.

2.6. RNA extraction, cDNA library construction, and sequencing

RNA extraction, preparation, and sequencing methods used in previous work were employed in this study (Qi et al., 2024). Total RNA was extracted using TRIzol reagent (TaKaRa, Dalian, China), and genomic DNA was eliminated using a DNase I RNase-free (TaKaRa) kit. The samples were incubated for 2 min at 42 °C. RNA quality and quantity were analyzed using a BioAnalyzer 2100 (Agilent Technology, Santa Clara, CA) and NanoDrop 2000 spectrophotometer (Infinigen Biotechnology Inc., City of Industry, CA), respectively. Only high-quality RNA samples (OD 260/280 ≥ 1.9, OD 260/230 ≥ 1.5, RIN ≥ 8.0) were used to construct sequencing library. After quality control, these RNAs were reverse transcribed into cDNAs. The intestinal tissue cDNA was subsequently subjected to 150 bp paired-end sequencing using the Illumina HiSeq TM 2500 platform (Illumina, USA) at Applied Protein Technology Co., Ltd. (Shanghai, China), while the bacterial cDNA was cryopreserved in liquid nitrogen for subsequent use.

For the assessment of bacterial virulence, bacterial RNA was independently extracted. Genomic DNA was eliminated and the RNA was reverse-transcribed into cDNA using a PrimeScript™ RT reagent Kit with gDNA Eraser (TaKaRa). Using bacterial cDNA as template, 8 virulence genes *exu* (nuclease), *ast* (cytotoxic enterotoxin), *alt* (thermolabile enterotoxins), *ser* (serine protease), *aer* (aerolysin), *act* (cytotoxic enterotoxins), *fla* (flagellin), and *lip* (lipase) were amplified by PCR. Primer sequences were designed according to Nawaz (Nawaz et al., 2010) (Table S1), with both primer synthesis and PCR product verification performed by Tsingke Biotechnology Co., Ltd. (Beijing, China).

2.7. Quality control, mapping, transcriptome assembly and annotation

Transcriptomic sequencing was performed using three independent biological replicates per treatment group. Raw sequencing reads (FASTQ format) were processed with Trimmomatic to remove adapters and low-quality bases. Clean reads were evaluated for sequencing quality by calculating error rates, Q20, Q30 scores, and GC content. HISAT2 v2.2.1 (Kim et al., 2015) was utilized to align the clean reads to the Chinese soft-shelled turtle reference genome (GCF_000230535.1; https://www.ncbi.nlm.nih.gov/assembly/GCF_000230535.1) (Wang et al., 2013) to generate read mapping statistics. Transcript assembly and annotation (including novel transcripts) were performed using StringTie2 v1.3.3b (Pertea et al., 2015) with reference genome guidance.

2.8. Differential expression genes and enrichment

Gene expression levels were quantified using the fragments per kilobase per million mapped fragments (FPKM) method, which inherently serves as an intra-sample normalization technique by correcting for both sequencing depth and transcript length. Subsequently, differential expression analysis, including robust inter-sample normalization, was performed using the DESeq2 R package (Love et al., 2014). Differentially expressed genes (DEGs) were identified with a > 2-fold change (|log2FC= ≥ 1) and an adjusted *p*-value < 0.05. Functional annotation of DEGs was performed using the Kyoto Encyclopedia of Genes and Genomes (KEGG) databases.

2.9. Gene expression levels were analyzed by quantitative real-time PCR (qRT-PCR)

The expression levels of complement and coagulation cascades genes (Table S2) were analyzed by quantitative qRT-PCR following the aforementioned protocol. The reaction system contained 2 μL of cDNA, 10 μL of TB Green Premix Ex Taq (Takara, Dalian, China), 0.5 μL of each primer, and RNase-free water to a final volume of 20 μL. The qRT-PCR program was run in the ABI StepOnePlus System (Applied Biosystems, Foster, Schaumburg, IL, USA) as follows: 95℃ for 30 s, followed by 40 cycles of 95℃ for 5 s, and 60℃ for 30 s, with a final step of 65°C for 1 s and 95°C for 15 s. Gene expression levels were normalized to the β-actin gene, and fold changes in mRNA levels between treatment and control groups were calculated using the $2^{-\Delta\Delta CT}$ method (Houghton and Cockerill, 2006).

2.10. Statistical analysis

To preclude subjective bias, all samples for histological (H&E),

apoptotic, qPCR, and biochemical and ELISA kit assays were anonymously coded prior to processing. The researchers performing the assays and extracting data remained completely blinded to treatment assignments, with unblinding occurring only prior to the final statistical evaluation. All statistical analyses were performed with the GraphPad Prism 7 software (GraphPad Software Inc., La Jolla, CA, USA). All continuous data are consistently presented as the mean ± standard error (SE) to accurately reflect biological variability. To identify appropriate statistical methods, the normality of data distribution was assessed using the Shapiro–Wilk test, and the homogeneity of variances was evaluated using Levene's test. For comparisons strictly between two independent groups, an unpaired Student's *t*-test was applied. For comparisons among three or more experimental groups, a One-way Analysis of Variance (ANOVA) was conducted, followed by Tukey's post hoc test to strictly correct for multiple comparisons. Statistical significance was defined as $p < 0.05$, $p < 0.01$, or $p < 0.001$.

3. Result

3.1. Antibacterial activity of AJ against A. veronii

As showed in Table S3, the MIC values of AJ against the *A. veronii* was 25 mg/mL. Based on MIC results, 100, 50, and 25 mg/mL concentrations were selected for MBC testing, with no bacterial growth observed on solid medium at 50 mg/mL (Fig. 1A).

Based on the MIC and MBC results, 25 mg/mL of AJ was used to assess its effect on *A. veronii* growth. At this concentration, the logarithmic growth phase of *A. veronii* was prolonged from 6 h to 15 h, and the growth rate remained consistently lower than that of the control group throughout the experiment. In contrast, the bacterial growth curve of the control group, which was not exposed to the drug solution, exhibited a characteristic S-shaped pattern, consistent with the typical growth behavior of *A. veronii* (Fig. 1B).

PCR amplification targeting eight virulence genes from the template DNA of *A. veronii* failed to amplify the *alt*, *ser*, and *lip* genes. Clear bands were observed in lanes 1, 2, 5, 6 and 7, corresponding to amplicon sizes of 323 bp, 331 bp, 431 bp, 232 bp and 608 bp, respectively (Fig. 1C). These sizes were consistent with the expected amplicons for the target genes, confirming the presence of five virulence factors: *exu*, *ast*, *aer*, *act* and *fla*. Further analysis demonstrated that at the MIC, expression of the five virulence genes *exu, ast, aer*, *act*, and *fla* was significantly down-regulated ($p < 0.05$) in the Av+AJ group compared to the control group. Notably, the expression of *exu* and *ast* was completely suppressed in the Av+AJ group (Fig. 1D).

3.2. Effects of AJ as a feed additive on the intestinal of Chinese soft-shelled turtle

To evaluate the effects of AJ as a dietary additive on the health status of Chinese soft-shelled turtles, a comparative analysis was performed between the control and AJ-supplemented groups. After 2 weeks of feeding, T-AOC activity was significantly higher ($p < 0.01$), while MPO and NO levels were significantly reduced ($p < 0.001$) in the group treated with 1250 mg/kg AJ extract compared to the control group (Fig. 2A–C). Additionally, the expression levels of IL-6 and IL-18 were significantly decreased in the 1250 mg/kg AJ-supplemented group compared to the control group ($p < 0.05$), while the level of intestinal sIgA was significantly increased (Fig. 2D–G; $p < 0.05$). Histological analysis of the intestine revealed well-defined and intact structures of the intestinal mucosa, lamina propria, and muscularis mucosae, with orderly arranged villi featuring prominent central lacteals within the lamina propria, in both groups of Chinese soft-shelled turtles (Fig. 4A and B). Concurrently, TUNEL assays showed a decrease in intestinal cell apoptosis in the AJ-supplemented group relative to the control group, although the difference was not statistically significant (Fig. 5; $p > 0.05$). These findings indicated that AJ supplementation may contribute to maintaining intestinal health by enhancing antioxidant capacity, reducing the expression of inflammatory factors, and mitigating cell apoptosis.

3.3. The protective effect of group AJ against A. veronii infection on Chinese soft-shelled turtle

To evaluate the protective efficacy of AJ on Chinese soft-shelled

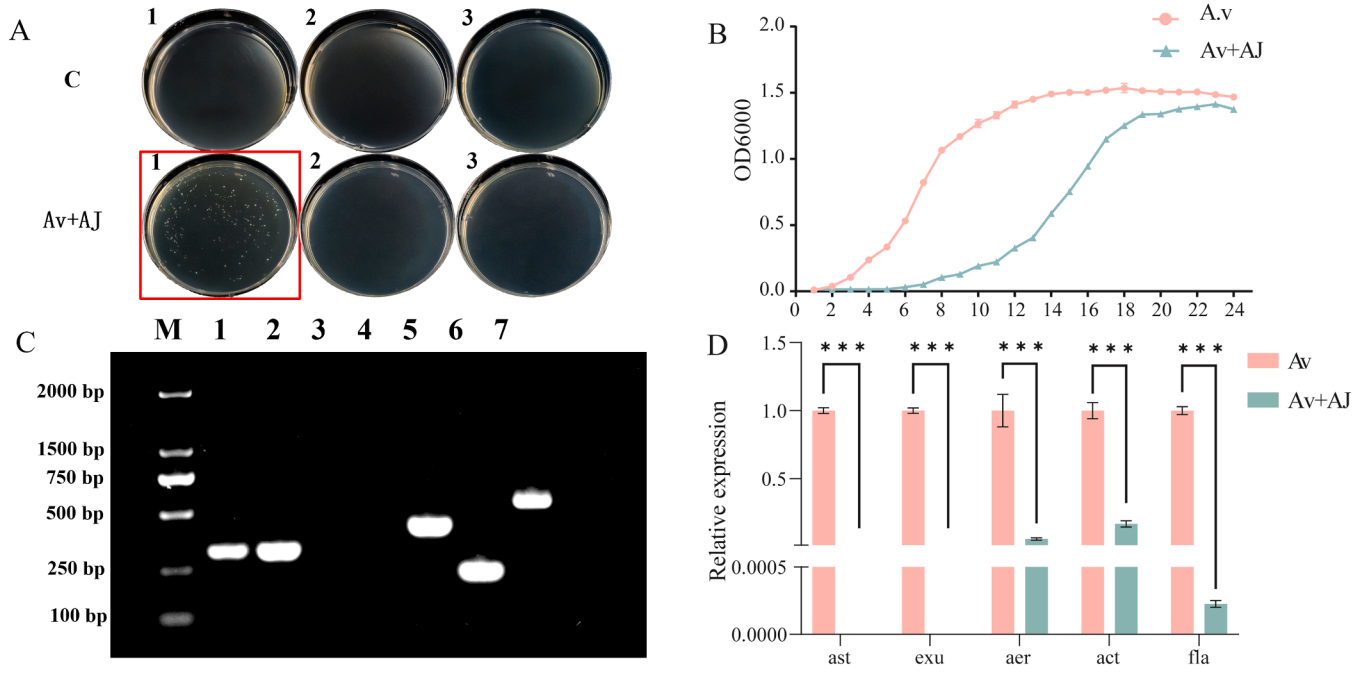

Fig. 1. (A) Minimum bactericidal concentration of AJ extract against *A. veronii* after 24 h; (B) Effect of AJ on the growth curve of *A. veronii*; (C) PCR amplification, confirmation and screening of *A. veronii* virulence genes; (D) Effect of AJ on the expression of *A. veronii* virulence genes; * Represents significant differences: * $p < 0.05$; ** $p < 0.01$; *** $p < 0.001$.

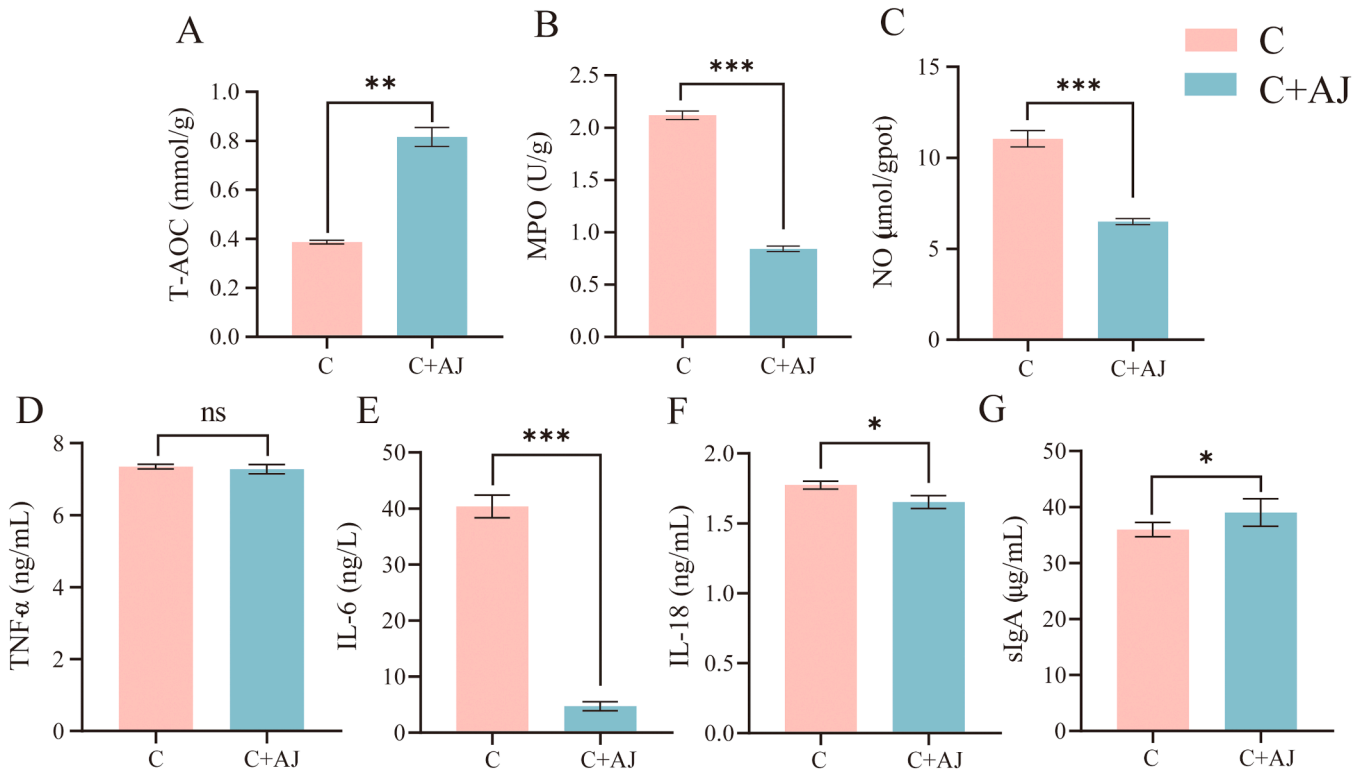

Fig. 2. Safety evaluation of AJ on intestinal parameters in healthy Chinese soft-shelled turtles. Data are shown for (A) T-AOC, (B) MPO, (C) NO, (D) TNF-α, (E) IL-6, (F) IL-18 and (G) sIgA. All data are represented as mean ± SE (n = 3). T-AOC: total antioxidant capacity; MPO: myeloperoxidase; NO: nitric oxide; TNF-α: tumor necrosis factor-α; IL-6: interleukin-6; IL-18: interleukin-18; sIgA: secretory immunoglobulin A. * Represents significant differences: * $p < 0.05$; ** $p < 0.01$; *** $p < 0.001$.

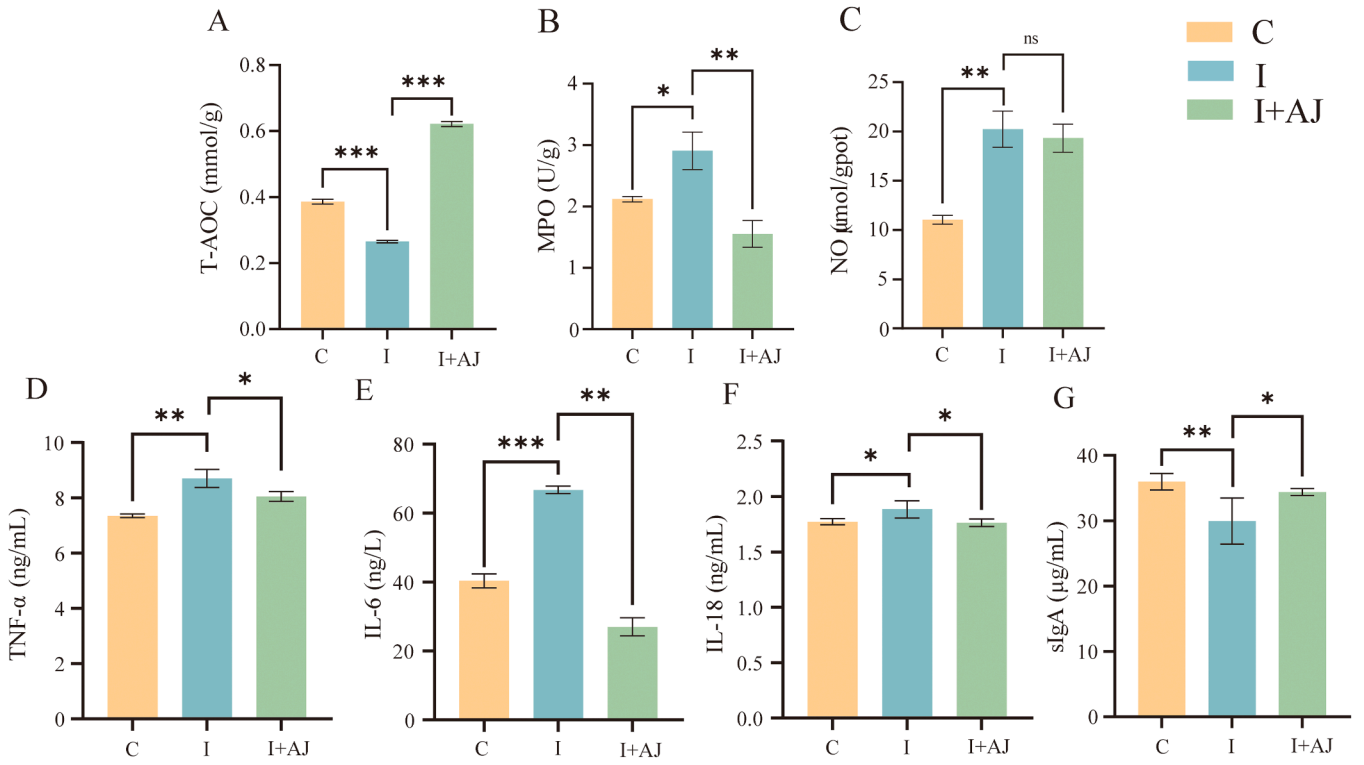

Fig. 3. Protective effects of AJ supplementation against *A. veronii*-induced intestinal oxidative stress and inflammation. Data are shown for (A) T-AOC, (B) MPO, (C) NO, (D) TNF-α, (E) IL-6, (F) IL-18 and (G) sIgA. All data are represented as mean ± SE (n = 3). T-AOC: total antioxidant capacity; MPO: myeloperoxidase; NO: nitric oxide; TNF-α: tumor necrosis factor-α; IL-6: interleukin-6; IL-18: interleukin-18; sIgA: secretory immunoglobulin A. * Represents significant differences: * $p < 0.05$; ** $p < 0.01$; *** $p < 0.001$.

turtles, we assessed its impact on mortality rates, non-specific immunity, inflammatory cytokine levels, histopathological changes, and cellular apoptosis. In the control group, the mortality rate of *A. veronii*-infected turtles reached 60% within one week post-infection, whereas dietary supplementation with AJ (the I+AJ group) significantly reduced the mortality rate to 20% (Table S4).

Non-specific immune assays demonstrated that the T-AOC activity in Group I was significantly lower than in Group C, whereas the I+AJ group exhibited significantly higher T-AOC activity compared to I group (Fig. 3A; $p < 0.001$). MPO activity showed a significant elevation in Group I relative to Group C ($p < 0.05$), but was markedly reduced in the I+AJ group compared to Group I (Fig. 3B; $p < 0.01$). NO levels increased significantly in Group I compared to Group C ($p < 0.01$), while the I+AJ group demonstrated a decreasing trend in NO content but no significance (Fig. 3C; $p > 0.05$).

Analysis of intestinal pro-inflammatory cytokines revealed that compared to Group C, TNF-α, IL-6, and IL-18 expression levels were significantly elevated in Group I (Fig. 3D–F; $p < 0.05$). These inflammatory cytokines were significantly downregulated in the I+AJ group relative to Group I (Fig. 3D–F; $p < 0.05$). Intestinal sIgA content was significantly lower in Group I compared to both Group C and the I+AJ group (Fig. 3G; $p < 0.05$).

Histological analysis revealed that *A. veronii* infection caused disruption of intestinal striated border structures and intensely stained mucosal epithelial cells in Chinese soft-shelled turtles (Fig. 4C and D). In the I group, severe intestinal damage was observed, including structural blurring of intestinal architecture, disintegration and sloughing of mucosal and submucosal layers, abundant luminal mucosal debris, pyknotic nuclei, cellular lysis, absence of central lacteals, and inflammatory cell infiltration (Fig. 4C). In contrast, the I+AJ group exhibited markedly attenuated pathological alterations (Fig. 4D). Concurrently, TUNEL assay demonstrated that intestinal tissue apoptosis levels were significantly decrease in the I+AJ group compared to the I group (Fig. 5, Fig S2; $p < 0.01$).

3.4. Transcriptomic analysis of the intestine following infection with *A. veronii*

After sequence assembly and quantitative analysis of clean reads, a total of 4358 expressed genes were identified, including 1729 upregulated and 2629 downregulated genes (Fig S1A). KEGG enrichment analysis of differentially expressed genes (DEGs) annotated 222 DEGs to

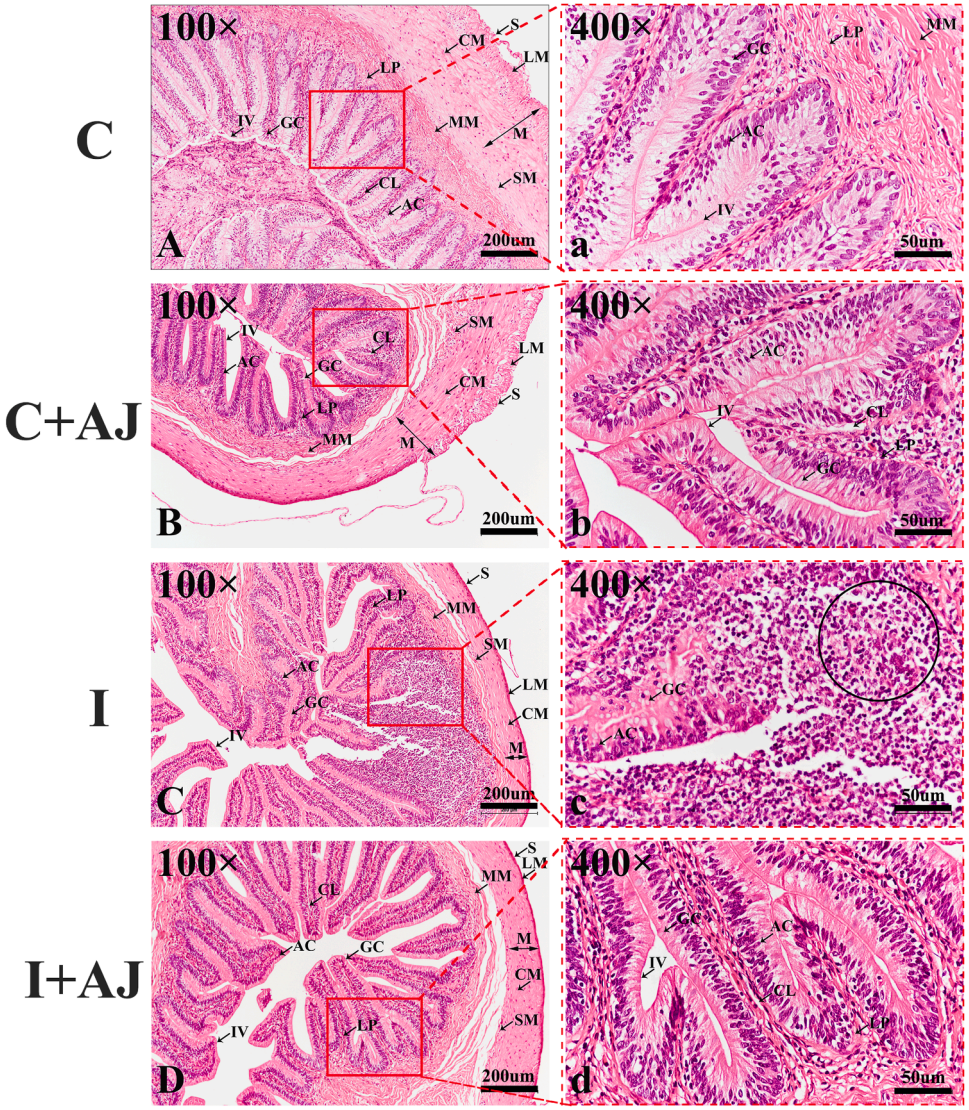

Fig. 4. Images of intestinal morphology observed using an optical microscope. (A, B, C, D) represent magnification at 100 × , and (a, b, c, d) represent magnification at 400 × . S: Serosa; M: Muscular layer; LM: Longitudinal muscle; CM: Circular muscle; SM: Submucosa; MM: Muscularis mucosae; LP: Lamina propria; IV: Intestinal villi; CL: Central lacteal; GC: Goblet cells; AC: Absorptive cells; ○: Inflammatory cell infiltration; Scale bars in A–D: 200 μm; Scale bars in a–d: 50 μm.

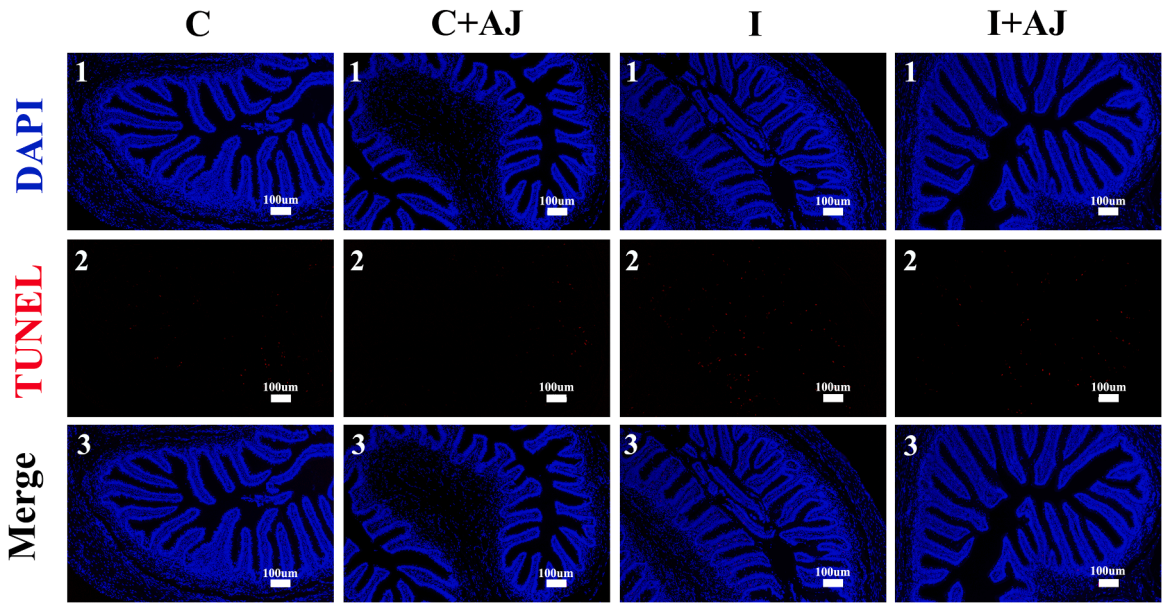

Fig. 5. TUNEL assay for detecting apoptosis of intestinal cells in Chinese soft-shelled turtles. Representative images of the Control (C), Control + AJ (C+AJ), Infected (I), and Infected + AJ (I+AJ) groups are shown in columns from left to right. For each group: panels in row 1 show DAPI staining for cell nuclei (blue); panels in row 2 show TUNEL staining for apoptotic cells (red); panels in row 3 show the merged images. Scale bars = 100 μm.

210 signaling pathways, with the top 20 enriched signaling pathways presented (Fig S1B). To investigate immune response mechanisms in Chinese soft-shelled turtle post-*A. veronii* infection, six immune-related pathways were prioritized: complement and coagulation cascades (CCC), toll-like receptor signaling pathway, platelet activation, NOD-like receptor signaling pathway, apoptosis, and natural killer cell-mediated cytotoxicity, and the CCC pathway showed the most significant enrichment (Table S5). Subsequently, we screened for genes related to the complement and coagulation cascades from the DEGs. We found that *F3*, *LOC102451598*, *LOC102449075*, *LOC102461035* and *F2RL2* were significantly upregulated in Group C, whereas a total of 14 genes, including *FGB*, *F5*, *FGG* and *C9*, were upregulated in Group I. To visualize these results, expression heatmaps of the complement and coagulation cascade-related DEGs across experimental groups were generated (Fig. 6A).

3.5. *Effects of AJ on gene expression in the coagulation cascade pathway*

Quantitative RT-qPCR validation revealed distinct expression differences of these DEGs in Groups C, I, and I+AJ. The expression levels of *C3*, *F3*, *F5*, *FGG* and *C9* showed progressive increases across the three groups, with I+AJ exhibiting significant upregulation compared to Group I ($p < 0.05$, Fig. 6B). *F2RL2* expression initially decreased then significantly increased, while *ITGB2* displayed an inverse pattern with an initial significant elevation followed by marked reduction ($p < 0.05$, Fig. 6B). *LOC102454598* demonstrated a non-significant downward trend across groups, and *LOC102461035* showed significant initial downregulation followed by non-significant recovery (Fig. 6B). To visually illustrate these expression dynamics within the CCC signaling pathway, we annotated the corresponding gene expression trends onto its schematic and simplified the diagram by retaining only nodes enriched with DEGs. The simplified pathway diagram reveals that following *A. veronii* stimulation in intestinal tissue, *F3* in the coagulation

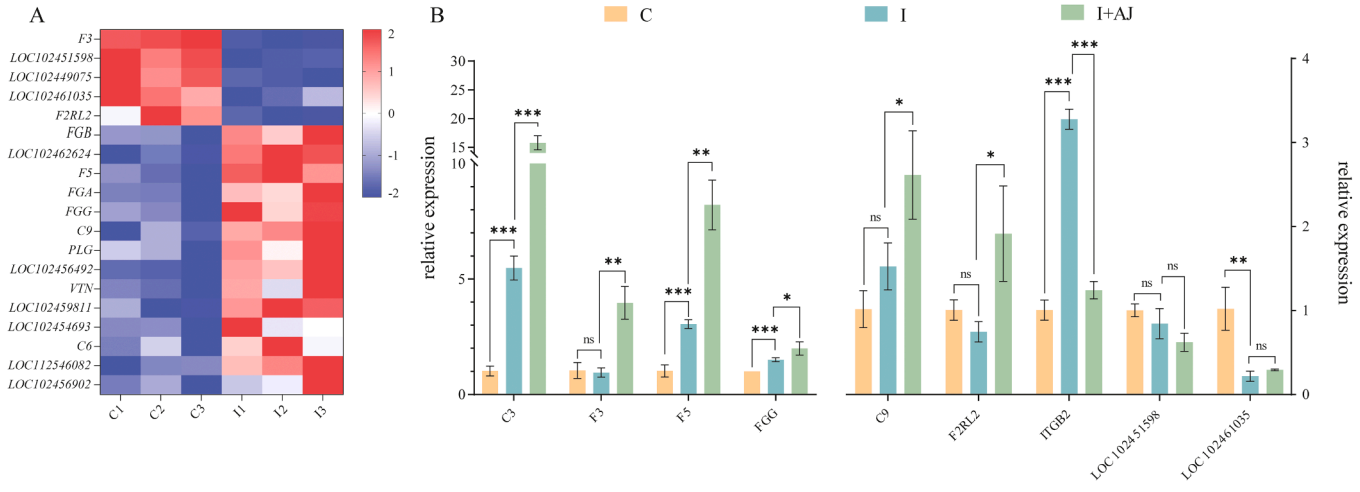

Fig. 6. (A) Heatmap of differentially expressed genes (DEGs) enriched in the complement and coagulation cascades. Each column represents a sample, and each row represents a gene. Red indicates upregulation, and blue indicates downregulation. (B) Effect of AJ on the expression of genes involved in the complement and coagulation cascades in Chinese soft-shelled turtles infected with *A. veronii*.

cascade activates *F10*, and the activated *F5/F10* complex catalyzes the conversion of *F2* (prothrombin) to thrombin. Thrombin subsequently cleaves fibrinogen (*FIB*) to form fibrin, promoting coagulation to confine pathogen dissemination. Additionally, thrombin triggers inflammatory responses via *PAR* receptor activation (Fig. 7). Within the complement cascade pathway, the core component *C3* collaborates with regulatory proteins to defend against pathogens. This defense primarily involves the assembly of the membrane attack complex (MAC) from *C5b* and *C9*, countering *A. veronii* invasion.

4. Discussion

Although Chinese herbal medicines demonstrate immense potential for preventing bacterial diseases in aquaculture, their development and application remain highly complex (Tadese et al., 2022). To date, while bacterial diseases in Chinese soft-shelled turtles have been extensively investigated (Chen et al., 2024; Zhou et al., 2011), empirical evidence regarding both the antibacterial efficacy of AJ and its protective benefits on intestinal health as a dietary supplement remains limited. Therefore, the present study first evaluated the in vitro antibacterial activity of AJ against *Aeromonas veronii* (*A. veronii*). Subsequently, we investigated its modulatory effects on the intestinal health of Chinese soft-shelled turtles as a feed additive, as well as its protective efficacy against *A. veronii* infection.

A. veronii employs extracellular enzymes and toxins during host infection to subvert primary defenses, facilitate invasion, and exacerbate severity (Nawaz et al., 2010; Song et al., 2004). Notably, not all *A. veronii* strains possess all virulence genes (Nawaz et al., 2010). A total of five critical virulence genes were identified in our isolated strain: *act*, *aer*, *ast*, and *exu*, which encode pore-forming hemolysins that lyse host cells, along with *fla*, which governs flagellar motility essential for adhesion and invasion (Beaz-Hidalgo and Figueras, 2013; Merino et al., 2014; Whitesides, 2006). Previous gene knockout studies confirm that these virulence factors are indispensable for bacterial proliferation and infectivity (Lebkowski et al., 2020; Yang et al., 2020, 2019). Consistent with this, our in vitro data (MIC, MBC, and growth curves) demonstrated that AJ treatment significantly inhibited *A. veronii* growth. Concurrently, AJ significantly suppressed the expression of these five virulence genes ($p < 0.05$). Therefore, our results reveal that AJ can inhibit bacterial growth and reproduction by suppressing the expression of virulence genes of *A. veronii*.

Non-specific immunity parameters are frequently utilized to evaluate organismal health (Netea et al., 2019). Specifically, T-AOC reflects the antioxidant defense capacity (Fei et al., 2024; Zhou et al., 2016), whereas elevated MPO and NO levels serve as established biomarkers for tissue inflammation (Lefer and Lefer, 1999; Lehrer and Cline, 1969; Li et al., 2008). Additionally, secretory IgA (sIgA) acts as the first line of defense in maintaining mucosal homeostasis (Li et al., 2020; Maningas et al., 2013). Although the anti-inflammatory, antioxidant, and immunomodulatory properties of AJ have been well-documented in various human and animal models (Lee et al., 2022; Oh et al., 2022), its application in aquaculture remains limited. In the present study, dietary supplementation with 1250 mg/kg AJ significantly increased intestinal T-AOC and sIgA levels while reducing MPO and NO activities in Chinese soft-shelled turtles. Taken together, these findings demonstrate that AJ effectively promotes intestinal health by mitigating oxidative stress and inflammation, while reinforcing the mucosal immune barrier.

Accumulated evidence suggest that inflammation and intestinal barrier dysfunction are primary pathological features of *A. veronii* infection in Chinese soft-shelled turtles (Hu et al., 2023). The intestinal epithelium, the largest host-environment interface, serves as a crucial barrier that selectively restricts the penetration of toxins and antigens, while also facilitating the absorption of nutrients and water (Buckley and Turner, 2018; Turner, 2009). Moreover, the crosstalk between this barrier and local intestinal immunity dictates the pathogenesis of infection (Shi et al., 2020). Barrier disruption overactivates intestinal immunity, triggering a massive release of pro-inflammatory cytokines (IL-18, IL-6, and TNF-α) that exacerbates tissue injury (Kaminsky et al., 2021). Concurrently, severe inflammation and oxidative stress synergistically drive excessive apoptosis, ultimately leading to organ failure (Chen et al., 2023; Zhang et al., 2023; Zhu et al., 2023). Furthermore, because severe inflammation is inversely correlated with the barrier integrity required for regulating sIgA secretion, mitigating oxidative and inflammatory damage is vital for preserving mucosal defenses (Li et al., 2020; Ma, 1997). Therefore, enhancing intestinal antioxidant capacity and mitigating excessive inflammation can reduce tissue damage, preserve sIgA secretion, and lower apoptosis levels, ultimately slowing disease progression (Liang et al., 2024). Notably, our study

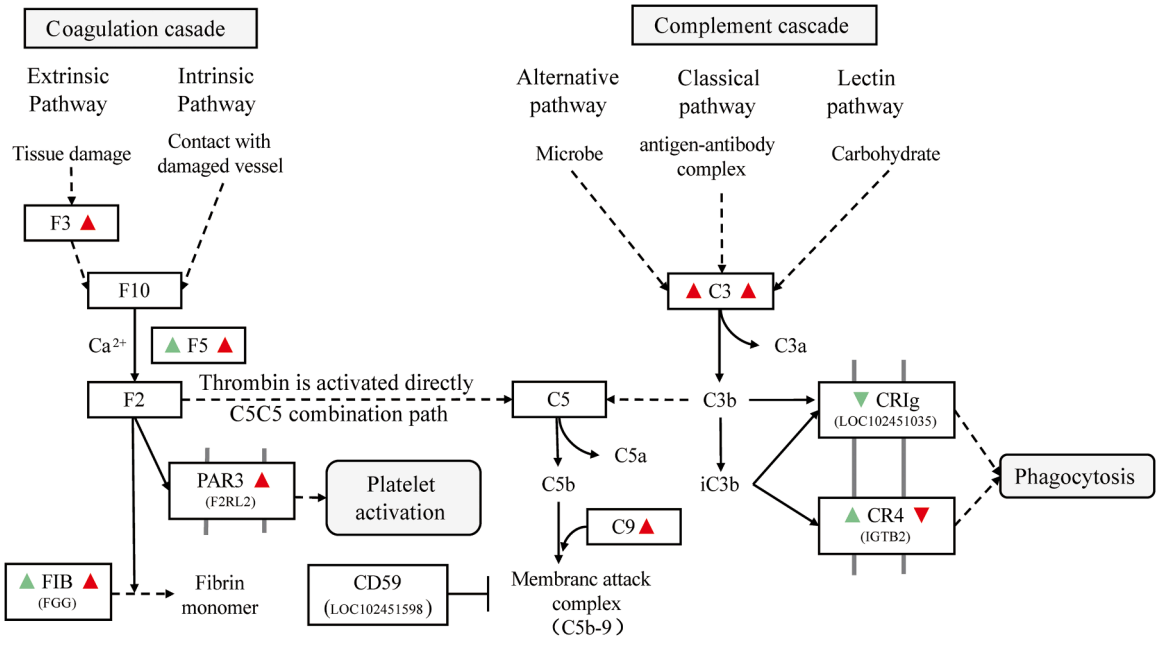

Fig. 7. Effect of AJ on gene expression within the complement and coagulation cascades of Chinese soft-shelled turtles. Within each box, the left arrow indicates the up- or down-regulation of the gene in group I compared to group C, while the right arrow indicates its expression change in the I+AJ group compared to group I.

demonstrated that AJ supplementation significantly elevated T-AOC activity and suppressed pro-inflammatory cytokine expression in *A. veronii*-infected turtles. Consequently, AJ effectively preserved intestinal barrier integrity and sIgA secretory function, suggesting that the protective effect of AJ against *A. veronii* is related to its anti-inflammatory and antioxidant effects.

A. veronii infections frequently progress to sepsis, a condition to which bacterial serine proteases may contribute by degrading fibrinogen and inducing hemorrhagic tendencies (Imamura et al., 2008; Janda and Abbott, 1998). To counter this invasion, the complement and coagulation cascades (CCC) orchestrate a synergistic host defense (Ricklin et al., 2010; Walport, 2001), whereby complement activation facilitates pathogen clearance and membrane attack complex (MAC, C5b-9) formation (Huber-Lang et al., 2013; Mullereberhard, 1986), while coagulation factors entrap bacteria and generate antibacterial peptides (Frick et al., 2006; Nickel and Renne, 2012). Notably, enhanced CCC activity does not equate to improved efficacy. While these cascades are physiologically designed for localized defense, their systemic overactivation can seriously threaten the host (Huber-Lang et al., 2013). Consequently, these findings provide a strong rationale for using natural active substances at appropriate concentrations to effectively regulate this network. In our study, *A. veronii* infection induced a moderate CCC activation in the intestine ($p < 0.05$); notably, AJ supplementation at 1250 mg/kg significantly amplified this defense, upregulating *F3*, *F5*, *FGG*, *C3* and *C9* expression ($p < 0.01$) compared to the I group. Previous studies have shown that rhein, gallic acid, and emodin can activate complement pathways (Zhong et al., 2024). As AJ is rich in these active compounds, this composition may explain the enhanced CCC activation observed in our study. Furthermore, because dietary AJ significantly alleviated overall tissue damage, we propose that it may function as an immunostimulant to strengthen the intestinal CCC, thereby enhancing the resistance of Chinese soft-shelled turtles against *A. veronii* infection.

Several limitations of this study should be acknowledged. Specifically, the two-week feeding duration may not fully represent long-term physiological adaptations or potential immune tolerance associated with prolonged supplementation. Additionally, we have yet to pinpoint which specific active constituent within the complex AJ mixture primarily mediates the bacteriostatic action against *A. veronii*. Therefore, future studies focusing on extended feeding periods and active compound identification are required to fully elucidate the pharmacological profile of AJ in aquaculture.

5. Conclusions

Overall, the present study showed that AJ significantly inhibited the growth of *A. veronii* and the expression of its virulence genes at a concentration of 25 mg/mL. Dietary supplementation with AJ at 1250 mg/kg significantly enhanced intestinal antioxidant capacity and intestinal mucosal homeostasis. Following *A. veronii* infection, AJ supplementation significantly increased intestinal antioxidant capacity, decreased the expression of pro-inflammatory cytokines, and maintained intestinal barrier function, thereby reducing inflammatory damage in Chinese soft-shelled turtles. Furthermore, AJ may function as an immunostimulant by activating the intestinal complement and coagulation cascades, thereby triggering subsequent coagulation, inflammatory, and immune responses, and promoting MAC formation against *A. veronii* infection. These findings suggest that AJ could serve as a potential functional feed additive to enhance the resistance of Chinese soft-shelled turtles against *A. veronii* infection

Institutional review board statement

The authors declare that all experiments involving *Pelodiscus sinensis* were ethical. All of our experiments were conducted in compliance with the standard ethical guidelines and under the control of Nanchang University.

Author contributions

Yijiang Hong and Kou Peng designed the experiments. Jicheng Yang and Mengyuan Li performed the experiments. Jun Hu, Ruixiang Zhai, Shujie Guo, Zhirui Zhu, Beijuan Hu, Junhua Wang, Daxian Zhao and Zhongguo Li assisted in performing the experiments. Jicheng Yang and Mengyuan Li completed the writing of the manuscript. Yijiang Hong supervised this study, as well as revised the paper. All authors have read and agreed to the published version of the manuscript.

CRediT authorship contribution statement

Zhirui Zhu: Software, Investigation. **Shujie Guo:** Software, Investigation. **Beijuan Hu:** Resources, Formal analysis. **Kou Peng:** Resources, Funding acquisition, Conceptualization. **Yijiang Hong:** Writing – review & editing, Resources, Funding acquisition, Conceptualization. **Zhongguo Li:** Resources, Investigation. **Daxian Zhao:** Supervision, Resources. **Junhua Wang:** Supervision, Resources. **Ruixiang Zhai:** Investigation, Data curation. **Jun Hu:** Methodology, Investigation. **Mengyuan Li:** Writing – original draft, Methodology, Data curation. **Jicheng Yang:** Writing – original draft, Methodology, Formal analysis, Data curation.

Funding

This work was supported by the National Key Research and Development Program of China (2023YFD2401800), Jiangxi Provincial Major Science and Technology R&D Special Project (20233AAE02012), Jiangxi Provincial Joint Research Project on Aquatic Breeding (jxsczy202601, 2024yyzygg-03, 2022yyzygg-02), Jiangxi Province Famous, Special and High-quality Aquatic Products Research System (JXARS-15), the Natural Science Foundation of Jiangxi Province, China (20242BAB25399) and the Project of Jiangxi Provincial Agricultural (Nanfeng County Turtle and Soft-shelled Turtle) Science and Technology Complex (Fengfu Zi〔2024〕No. 49).

Declaration of Competing Interest

The authors declare that they have no known competing financial interests or personal relationships that could have appeared to influence the work reported in this paper.

Acknowledgments

We gratefully acknowledge Mr. Guohui Wu, Chairman of Jiangxi Tianpeng Eco-Agriculture Co., Ltd., for providing the Chinese soft-shelled turtle samples, and Dr. Yansheng Dong, Director of the Nanfeng County Turtle and Soft-shelled Turtle Hospital, for technical support.

Appendix A. Supporting information

Supplementary data associated with this article can be found in the online version at doi:10.1016/j.aqrep.2026.103676.

Data availability

Data will be made available on request.

References

Abd El-Gawad, E.A., El Asely, A.M., Soror, E.I., Abbass, A.A., Austin, B., 2020. Effect of dietary *Moringa oleifera* leaf on the immune response and control of *Aeromonas hydrophila* infection in Nile tilapia (*Oreochromis niloticus*) fry. Aquacult. Int. 28 (1), 389–402. https://doi.org/10.1007/s10499-019-00469-0.

AftabUddin, S., Siddique, M.A.M., Romkey, S.S., Shelton, W.L., 2017. Antibacterial function of herbal extracts on growth, survival and immunoprotection in the black

tiger shrimp *Penaeus monodon*. Fish. Shellfish Immunol. 65, 52–58. https://doi.org/10.1016/j.fsi.2017.03.050.
Amin, A., El Asely, A., Abd El-Naby, A.S., Samir, F., El-Ashram, A., Sudhakaran, R., Dawood, M.A.O., 2019. Growth performance, performance, intestinal histomorphology and growth-related gene expression in response to dietary *Ziziphus mauritiana* in Nile tilapia (*Oreochromis niloticus*). Aquaculture 512, 734301. https://doi.org/10.1016/j.aquaculture.2019.734301.
Beaz-Hidalgo, R., Figueras, M.J., 2013. Aeromonas spp. whole genomes and virulence factors implicated in fish disease. J. Fish. Dis. 36 (4), 371–388. https://doi.org/10.1111/jfd.12025.
Bondad-Reantaso, M.G., MacKinnon, B., Karunasagar, I., Fridman, S., Alday-Sanz, V., Brun, E., Le Groumellec, M., Li, A.H., Surachetpong, W., Karunasagar, I., Hao, B., Dall'Occo, A., Urbani, R., Caputo, A., 2023. Review of alternatives to antibiotic use in aquaculture. Rev. Aquac. 15 (4), 1421–1451. https://doi.org/10.1111/raq.12786.
Buckley, A., Turner, J.R., 2018. Cell biology of tight junction barrier regulation and mucosal disease. Cold Spring Harb. Perspect. Biol. 10 (1), a029314. https://doi.org/10.1101/cshperspect.a029314.
Chen, M.M., Xue, M.Y., Chen, J.T., Xiao, Z.D., Hu, X.W., Zhang, C.J., Jiang, N., Fan, Y.D., Meng, Y., Zhou, Y., 2024. Isolation, identification and characterization of *Aeromonas jandaei* from diseased Chinese soft-shell turtles. J. Fish. Dis. 47 (4), e13919. https://doi.org/10.1111/jfd.13919.
Chen, Y., Zhang, X., Yang, J., Feng, W., Deng, G., Xu, S., Guo, M., 2023. Extracellular vesicles derived from selenium-deficient MAC-T cells aggravated inflammation and apoptosis by triggering the endoplasmic reticulum (ER) stress/PI3K-AKT-mTOR pathway in bovine mammary epithelial cells. Antioxidants 12 (12), 2077. https://doi.org/10.3390/antiox12122077.
Chen, J.S., Zhu, N.Y., Kong, L., Bei, Y.J., Zheng, T.L., Ding, X.Y., He, Z.Y., 2014. First reported fatal (*Bacillus thuringiensis*) infections in Chinese soft-shelled turtles (*Trionyx sinensis*). Aquaculture 428 16–20. https://doi.org/10.1016/j.aquaculture.2014.02.018.
Dadar, M., Dhama, K., Vakharia, V.N., Hoseinifar, S.H., Karthik, K., Tiwari, R., Khandia, R., Munjal, A., Salgado-Miranda, C., Joshi, S.K., 2017. Advances in aquaculture vaccines against fish pathogens: global status and current trends. Rev. Fish. Sci. Aquac. 25 (3), 184–217. https://doi.org/10.1080/23308249.2016.1261277.
Dai, X.H., Hu, J., Jin, F., Wu, D., Jian, S.Q., Zahid, A., Hu, B.J., Hong, Y.J., 2022. Pathology and drug susceptibility study of an outbreak of bacterial pathogen infecting the Chinese soft-shelled turtle (*Pelodiscus sinensis*). Aquacult. Res. 53 (17), 5743–5752. https://doi.org/10.1111/are.16057.
Dien, L.T., Ngo, T.P.H., Nguyen, T.V., Kayansamruaj, P., Salin, K.R., Mohan, C.V., Rodkhum, C., Dong, H.T., 2022. Non-antibiotic approaches to combat motile *Aeromonas* infections in aquaculture: current state of knowledge and future perspectives. Rev. Aquac. 15 (1), 333–366. https://doi.org/10.1111/raq.12721.
Elumalai, P., Kurian, A., Lakshmi, S., Faggio, C., Esteban, M.A., Ringo, E., 2020. Herbal Immunomodulators in Aquaculture. Rev. Fish. Sci. & Aquac. 29 (1), 33–57. https://doi.org/10.1080/23308249.2020.1779651.
Engelmann, B., Massberg, S., 2013. Thrombosis as an intravascular effector of innate immunity. Nat. Rev. Immunol. 13 (1), 34–45.
Fei, S., Kang, J., Ou, M., Liu, H., Zhang, X., Luo, Q., Li, K., Chen, K., Zhao, J., 2024. Effects of essential amino acids supplementation in a low-protein diet on growth performance, intestinal health and microbiota of juvenile blotched snakehead (*Channa maculata*). Fish. Shellfish Immunol. 149, 109555. https://doi.org/10.1016/j.fsi.2024.109555.
Foley, J.H., Conway, E.M., 2016. Cross talk pathways between coagulation and inflammation. Circ. Res. 118 (9), 1392–1408. https://doi.org/10.1161/circresaha.116.306853.
Frick, I.-M., Akesson, P., Herwald, H., Morgelin, M., Malmsten, M., Nagler, D.K., Bjorck, L., 2006. The contact system -: a novel branch of innate immunity generating antibacterial peptides. EMBO J. 25 (23), 5569–5578. https://doi.org/10.1038/sj.emboj.7601422.
Gharaei, A., Jorjani, H.E., Harijani, J.M., Miandare, H.K., 2020. Effects of *Tribulus terrestris* extract on masculinization, growth indices, sex determination and steroid hormones level in Zebra fish (*Danio rerio*). Int. Aquat. Res. 12 (1), 22–29. https://doi.org/10.22034/iar(20).2020.670992.
Hoseinifar, S.H., Sun, Y.-Z., Zhou, Z., Van Doan, H., Davies, S.J., Harikrishnan, R., 2020. Boosting immune function and disease bio-control through environment-friendly and sustainable approaches in finfish aquaculture: herbal therapy scenarios. Rev. Fish. Sci. Aquac. 28 (3), 303–321. https://doi.org/10.1080/23308249.2020.1731420.
Houghton, S.G., Cockerill, F.R., 2006. Real-time PCR: overview and applications. Surgery 139 (1), 1–5. https://doi.org/10.1016/j.surg.2005.02.010.
Hu, X.W., Xiao, Z.D., Li, B., Xue, M.Y., Jiang, N., Fan, Y.D., Chen, P., Qi, F., Kong, X.H., Zhou, Y., 2023. Isolation, Identification, and Characterization of (*Aeromonas veronii*) from Chinese Soft-Shelled Turtle (*Trionyx sinensis*). Microorganisms 11 (5), 1304. https://doi.org/10.3390/microorganisms11051304.
Huber-Lang, M., Kovtun, A., Ignatius, A., 2013. The role of complement in trauma and fracture healing. Semin. Immunol. 25 (1), 73–78. https://doi.org/10.1016/j.smim.2013.05.006.
Imamura, T., Nitta, H., Wada, Y., Kobayashi, H., Okamoto, K., 2008. Impaired plasma clottability induction through fibrinogen degradation by ASP, a serine protease released from *Aeromonas sobria*. FEMS Microbiol. Lett. 284 (1), 35–42. https://doi.org/10.1111/j.1574-6968.2008.01184.x.
Janda, J.M., Abbott, S.L., 1998. Evolving concepts regarding the genus *Aeromonas*: an expanding panorama of species, disease presentations, and unanswered questions. Clin. Infect. Dis. 27 (2), 332–344. https://doi.org/10.1086/514652.
Kaminsky, L.W., Al-Sadi, R., Ma, T.Y., 2021. IL-1β and the intestinal epithelial tight junction barrier. Front. Immunol. 12, 767456. https://doi.org/10.3389/fimmu.2021.767456.
Kay, W.W., Buckley, J.T., Ishiguro, E.E., Phipps, B.M., Monette, J.P.L., Trust, T.J., 1981. Purification and disposition of a surface protein associated with virulence of aeromonas-salmonicida. J. Bacteriol. 147 (3), 1077–1084. https://doi.org/10.1128/jb.147.3.1077-1084.1981.
Kim, D., Langmead, B., Salzberg, S.L., 2015. HISAT: a fast spliced aligner with low memory requirements. U121 Nat. Methods 12 (4), 357. https://doi.org/10.1038/nmeth.3317.
Lebkowski, T., Wolanski, M., Oldziej, S., Flardh, K., Zakrzewska-Czerwinska, J., 2020. AfsK-Mediated Site-Specific Phosphorylation Regulates DnaA Initiator Protein Activity in *Streptomyces coelicolor*. J. Bacteriol. 202 (3), e00597–00519. https://doi.org/10.1128/jb.00597-19.
Lee, C.-L., Jhan, Y.-L., Chiang, H.-M., Chen, Y.-H., Chen, C.-J., Chang, Y.-S., 2022. Characterization of chemical constituents with their antioxidant and anti-melanogenesis activities from the roots of *Ampelopsis japonica*. Nat. Prod. Res. 36 (12), 3133–3137. https://doi.org/10.1080/14786419.2021.1939335.
Lefer, A.M., Lefer, D.J., 1999. Nitric oxide II. Nitric oxide protects in intestinal inflammation. Am. J. Physiol. -Gastrointest. Liver Physiol. 276 (3), G572–G575.
Lehrer, R.I., Cline, M.J., 1969. Leukocyte myeloperoxidase deficiency and disseminated candidiasis: the role of myeloperoxidase in resistance to Candida infection. J. Clin. Investig. 48 (8), 1478–1488. https://doi.org/10.1172/jci106114.
Li, X.-L., Cai, Y.-Q., Qin, H., Wu, Y.-J., 2008. Therapeutic effect and mechanism of proanthocyanidins from grape seeds in rats with TNBS-induced ulcerative colitis. Can. J. Physiol. Pharmacol. 86 (12), 841–849. https://doi.org/10.1139/y08-089.
Li, Y., Jin, L., Chen, T., 2020. The effects of secretory IgA in the mucosal immune system. Biomed. Res. Int. 2020, 2032057. https://doi.org/10.1155/2020/2032057.
Li, Y., Jin, L., Chen, T.X., 2020. The effects of secretory IgA in the mucosal immune system. Biomed. Res. Int. 2020, 2032057. https://doi.org/10.1155/2020/2032057.
Liang, J., Dai, W., Liu, C., Wen, Y., Chen, C., Xu, Y., Huang, S., Hou, S., Li, C., Chen, Y., Wang, W., Tang, H., 2024. Gingerenone A attenuates ulcerative colitis via targeting IL-17RA to inhibit inflammation and restore intestinal barrier function. Adv. Sci. 11 (28), e2400206. https://doi.org/10.1002/advs.202400206.
Liang, J.-H., Lin, H.-R., Yang, C.-S., Liaw, C.-C., Wang, I.C., Chen, J.-J., 2022. Bioactive components from *Ampelopsis japonica* with antioxidant, anti-α-glucosidase, and antiacetylcholinesterase activities. Antioxidants 11 (7). https://doi.org/10.3390/antiox11071228.
Lieke, T., Meinelt, T., Hoseinifar, S.H., Pan, B., Straus, D.L., Steinberg, C.E.W., 2020. Sustainable aquaculture requires environmental-friendly treatment strategies for fish diseases. Rev. Aquac. 12 (2), 943–965. https://doi.org/10.1111/raq.12365.
Liu, Q., Wen, J., Peng, Z., Liu, F., Tong, X., 2015. Review of the powder and decoction formulae in Traditional Chinese Medicine based on pharmacologically active substances and clinical evidence. J. Tradit. Chin. Med. 35 (3), 355–360.
Love, M.I., Huber, W., Anders, S., 2014. Moderated estimation of fold change and dispersion for RNA-seq data with DESeq2. Genome Biol. 15 (12). https://doi.org/10.1186/s13059-014-0550-8.
Lowry, R., Balboa, S., Parker, J.L., Shaw, J.G., 2014. *Aeromonas* flagella and colonisation mechanisms. In: Poole, R.K. (Ed.), Advances in microbial physiology, Advances in Bacterial Pathogen Biology, 65, pp. 203–256.
Ma, T.Y., 1997. Intestinal epithelial barrier dysfunction in Crohn's disease. Proc. Soc. Exp. Biol. Med. 214 (4), 318–327.
Maningas, M.B.B., Kondo, H., Hirono, I., 2013. Molecular mechanisms of the shrimp clotting system. Fish. Shellfish Immunol. 34 (4), 968–972.
Meng, X.M., Wang, L., Nikolic-Paterson, D.J., Lan, H.Y., 2025. Innate immune cells in acute and chronic kidney disease. Nat. Rev. Nephrol. 21 (7), 464–482. https://doi.org/10.1038/s41581-025-00958-x.
Merino, S., Wilhelms, M., Tomas, J.M., 2014. Role of *Aeromonas hydrophila* flagella glycosylation in adhesion to Hep-2 cells, biofilm formation and immune stimulation. Int. J. Mol. Sci. 15 (12), 21935–21946. https://doi.org/10.3390/ijms151221935.
Mullereberhard, H.J., 1986. The membrane attack complex of complement. Annu. Rev. Immunol. 4, 503–528. https://doi.org/10.1146/annurev.iy.04.040186.002443.
Nawaz, M., Khan, S.A., Khan, A.A., Sung, K., Tran, Q., Kerdahi, K., Steele, R., 2010. Detection and characterization of virulence genes and integrons in *Aeromonas veronii* isolated from catfish. Food Microbiol. 27 (3), 327–331. https://doi.org/10.1016/j.fm.2009.11.007.
Netea, M.G., Schlitzer, A., Placek, K., Joosten, L.A.B., Schultze, J.L., 2019. Innate and Adaptive Immune Memory: an Evolutionary Continuum in the Host's Response to Pathogens. Cell Host Microbe 25 (1), 13–26. https://doi.org/10.1016/j.chom.2018.12.006.
Nickel, K.F., Renne, T., 2012. Crosstalk of the plasma contact system with bacteria. Thromb. Res. 130, S78–S83. https://doi.org/10.1016/j.thromres.2012.08.284.
Oh, Y., Lee, H., Yang, B., Kim, S., Jeong, H., Kim, H., 2022. Anti-inflammatory Effects of *Ampelopsis Japonica* Root on Contact Dermatitis in Mice. Chin. J. Integr. Med. 28 (8), 719–724. https://doi.org/10.1007/s11655-022-3517-0.
Pertea, M., Pertea, G.M., Antonescu, C.M., Chang, T.-C., Mendell, J.T., Salzberg, S.L., 2015. StringTie enables improved reconstruction of a transcriptome from RNA-seq reads. Nat. Biotechnol. 33 (3), 290. https://doi.org/10.1038/nbt.3122.
Qi, M., Liu, W., Li, W., Chen, G., Shi, W., Yao, G., Bei, Y., Yuan, F., Meng, Q., Zhou, F., Ma, W., Ding, X., Zheng, T., 2024. Integrative transcriptomics and metabolomics analysis provide insight into the formation of skin pigmentation diversity in Chinese soft-shelled turtle (*Pelodiscus sinensis*). Aquaculture 593, 741344. https://doi.org/10.1016/j.aquaculture.2024.741344.
Ricklin, D., Hajishengallis, G., Yang, K., Lambris, J.D., 2010. Complement: a key system for immune surveillance and homeostasis. Nat. Immunol. 11 (9), 785–797. https://doi.org/10.1038/ni.1923.

Schuhladen, K., Roether, J.A., Boccaccini, A.R., 2019. Bioactive glasses meet phytotherapeutics: The potential of natural herbal medicines to extend the functionality of bioactive glasses. Biomaterials 217, 119288. https://doi.org/10.1016/j.biomaterials.2019.119288.

Sen, K., Lye, D., 2007. Importance of flagella and enterotoxins for *Aeromonas* virulence in a mouse model. Can. J. Microbiol. 53 (2), 261–269. https://doi.org/10.1139/w06-095.

Shi, Y.H., Vistro, W.A., Bai, X.B., Wu, R.Z., Chen, C., Huang, Y.F., Fazlani, S.A., Tarique, I., Yang, P., Chen, Q.S., 2020. Effect of seasonal variance on intestinal epithelial barriers and the associated innate immune response of the small intestine of the Chinese soft-shelled turtles. Fish. Shellfish Immunol. 97, 173–181. https://doi.org/10.1016/j.fsi.2019.12.042.

Song, T.Y., Toma, C., Nakasone, N., Iwanaga, M., 2004. Aerolysin is activated by metalloprotease in *Aeromonas veronii* biovar sobria. J. Med. Microbiol 53 (6), 477–482. https://doi.org/10.1099/jmm.0.05405-0.

Tadese, D.A., Song, C., Sun, C., Liu, B., Liu, B., Zhou, Q., Xu, P., Ge, X., Liu, M., Xu, X., Tamiru, M., Zhou, Z., Lakew, A., Kevin, N.T., 2022. The role of currently used medicinal plants in aquaculture and their action mechanisms: a review. Rev. Aquac. 14 (2), 816–847. https://doi.org/10.1111/raq.12626.

Turner, J.R., 2009. Intestinal mucosal barrier function in health and disease. Nat. Rev. Immunol. 9 (11), 799–809. https://doi.org/10.1038/nri2653.

Walport, M.J., 2001. Advances in immunology: Complement (First of two parts). N. Engl. J. Med. 344 (14), 1058–1066. https://doi.org/10.1056/nejm200104053441406.

Wang, Z., Pascual-Anaya, J., Zadissa, A., Li, W., Niimura, Y., Huang, Z., Li, C., White, S., Xiong, Z., Fang, D., Wang, B., Ming, Y., Chen, Y., Zheng, Y., Kuraku, S., Pignatelli, M., Herrero, J., Beal, K., Nozawa, M., Li, Q., Wang, J., Zhang, H., Yu, L., Shigenobu, S., Wang, J., Liu, J., Flicek, P., Searle, S., Wang, J., Kuratani, S., Yin, Y., Aken, B., Zhang, G., Irie, N., 2013. The draft genomes of soft-shell turtle and green sea turtle yield insights into the development and evolution of the turtle-specific body plan. Nat. Genet. 45 (6), 701. https://doi.org/10.1038/ng.2615.

Whitesides, G.M., 2006. The origins and the future of microfluidics. Nature 442 (7101), 368–373. https://doi.org/10.1038/nature05058.

Xiao, Z.D., Hu, X.W., Chen, J.T., Xue, M.Y., Zhang, C.J., Jiang, N., Liu, X.D., Fan, Y.D., Kong, X.H., Zhou, Y., 2024. Isolation and characterization of Bacillus cereus virulent phage CA1. Aquaculture 589 (3), 740989. https://doi.org/10.1016/j.aquaculture.2024.740989.

Yang, B., Song, H., An, D., Zhang, D., Raza, S.H.A., Wang, G., Shan, X., Qian, A., Kang, Y., Wang, C., 2020. Functional analysis of *preA* in *Aeromonas veronii* TH0426 reveals a key role in the regulation of virulence and resistance to oxidative stress. Int. J. Mol. Sci. 21 (1), 98. https://doi.org/10.3390/ijms21010098.

Yang, B., Zhang, D., Wu, T., Zhang, Z., Raza, S.H.A., Schreurs, N., Zhang, L., Yang, G., Wang, C., Qian, A., Kang, Y., Shan, X., 2019. Maltoporin (LamB protein) contributes to the virulence and adhesion of *Aeromonas veronii* TH0426. J. Fish. Dis. 42 (3), 379–389. https://doi.org/10.1111/jfd.12941.

Zhai, J.L., Xiao, Z.D., Xue, M.Y., Fan, Y.D., Meng, Y., Liu, W., Hu, X.W., Xing, Y.Y., Jiang, N., Zhou, Y., 2024. *Morganella morganii*, a bacterial pathogen in diseased Chinese soft-shelled turtles (*Pelodiscus sinensis*). Aquaculture 579, 740190. https://doi.org/10.1016/j.aquaculture.2023.740190.

Zhang, Y., Cui, J., Li, K., Xu, S., Yin, H., Li, S., Gao, X.-j, 2023. Trimethyltin chloride exposure induces apoptosis and necrosis and impairs islet function through autophagic interference. Ecotoxicol. Environ. Saf. 267, 115628. https://doi.org/10.1016/j.ecoenv.2023.115628.

Zhang, W.N., Zhao, J.P., Ma, Y.F., Li, J., Chen, X.H., 2022. The effective components of herbal medicines used for prevention and control of fish diseases. Fish. Shellfish Immunol. 126, 73–83. https://doi.org/10.1016/j.fsi.2022.05.036.

Zhong, L., Sun, J., Li, S., Qi, Y., Luo, M., Dong, L., Chen, J., 2024. Scorch processing of rhubarb (*Rheum* tanguticum Maxim. ex Balf.) pyrolyzed anthraquinone glucosides into aglycones and improved the therapeutic effects on thromboinflammation via regulating the complement and coagulation cascades pathway. J. Ethnopharmacol. 333, 118475. https://doi.org/10.1016/j.jep.2024.118475.

Zhou, C.L., Na, L.X., Shan, R.Q., Cheng, Y., Li, Y., Wu, X.Y., Sun, C.H., 2016. Dietary Vitamin C intake reduces the risk of type 2 diabetes in Chinese adults: HOMA-IR and T-AOC as potential mediators. Plos One 11 (9), e0163571. https://doi.org/10.1371/journal.pone.0163571.

Zhou, X.X., Wang, L., Feng, H., Guo, Q.L., Dai, H.P., 2011. Acute phase response in Chinese soft-shelled turtle (*Trionyx sinensis*) with *Aeromonas hydrophila* infection. Dev. Comp. Immunol. 35 (4), 441–451. https://doi.org/10.1016/j.dci.2010.11.011.

Zhu, M.-r, Wang, H.-r, Han, F.-x, Cai, Z.-l, Wang, J.-j, Guo, M.-y, 2023. Polyethylene microplastics cause apoptosis via the MiR-132/CAPN axis and inflammation in carp ovarian. Aquat. Toxicol. 265, 106780. https://doi.org/10.1016/j.aquatox.2023.106780.

Zhu, H., Wu, Y., Zhuang, Z., Xu, J., Chen, F., Wang, Q., Tang, Q., 2024. *Ampelopsis japonica* aqueous extract improves ovulatory dysfunction in PCOS by modulating lipid metabolism. Biomed. Pharmacother. 170. https://doi.org/10.1016/j.biopha.2023.116093.